

Prediction of the Bonding States of Cysteines Using the Support Vector Machines Based on Multiple Feature Vectors and Cysteine State Sequences

Yu-Ching Chen,¹ Yeong-Shin Lin,² Chih-Jen Lin,³ and Jenn-Kang Hwang^{1,2*}

¹*Institute of Bioinformatics, National Chiao Tung University, HsinChu, Taiwan, ROC*

²*Department of Biological Science and Technology, National Chiao Tung University, HsinChu, Taiwan, ROC*

³*Department of Computer Science, National Taiwan University, Taipei, Taiwan, ROC*

ABSTRACT The support vector machine (SVM) method is used to predict the bonding states of cysteines. Besides using local descriptors such as the local sequences, we include global information, such as amino acid compositions and the patterns of the states of cysteines (bonded or nonbonded), or cysteine state sequences, of the proteins. We found that SVM based on local sequences or global amino acid compositions yielded similar prediction accuracies for the data set comprising 4136 cysteine-containing segments extracted from 969 nonhomologous proteins. However, the SVM method based on multiple feature vectors (combining local sequences and global amino acid compositions) significantly improves the prediction accuracy, from 80% to 86%. If coupled with cysteine state sequences, SVM based on multiple feature vectors yields 90% in overall prediction accuracy and a 0.77 Matthews correlation coefficient, around 10% and 22% higher than the corresponding values obtained by SVM based on local sequence information. *Proteins* 2004;55:1036–1042. © 2004 Wiley-Liss, Inc.

Key words: support vector machines; disulfide bonds; cysteine state sequences; multiple feature vectors

INTRODUCTION

The oxidation states of cysteines play a key role in both protein structure and function.^{1–8} Cysteines form disulfide bridges to stabilize folded states by increasing favorable enthalpy interactions in the folded states and by lowering the entropy of the unfolded states.⁹ The capability to accurately predict the disulfide bonding states in proteins will be useful in the study of protein stability¹⁰ or functions,¹¹ and in the prediction of three-dimensional (3D) protein structures.¹² A number of computational approaches^{13–17} were developed to predict the bonding states of cysteines. Muskal et al.¹³ obtained 81% prediction accuracy by using neural networks based on the sliding windows that include the flanking amino acids of the centered cysteines. Fiser et al.,¹⁴ exploiting the difference between the sequential environments of free cysteine and bonded cystine, developed a statistical approach that yielded a much lower 71% prediction accuracy, though using a data set four times bigger. Fariselli et al.¹⁸ included evolutionary information in the form of multiple

sequence alignment and used a jury of neural networks to obtain 81% prediction accuracy. Later, Fiser and Simon,¹⁵ observing that cysteines of a protein tend to occur in the same oxidation states, developed a method based on multiple sequence alignments and achieved 82% prediction accuracy. Martelli et al.^{16,19} used the hidden neural networks (HNNs) developed by Krogh and Riis,²⁰ and obtained an overall prediction accuracy of 88%. Mucchielli-Giorgi et al.¹⁷ found that the amino acid content of the whole protein appears to be more informative about the disulfide bonding state than the local sequence window does. Using a combination of logistic functions learned with subsets of proteins homogeneous in terms of their amino acid content, they were able to obtain prediction accuracy close to 84% for 869 chains. The support vector machine (SVM) method²¹ has recently become popular in computational biology.^{22–26} We have previously successfully applied the SVM based on multiple feature vectors to protein fold assignment²⁶ and subcellular localization prediction.²⁷ In this work, we developed an approach to predict the bonding states of cysteines using SVM based on multiple feature vectors and the cysteine state sequences.

METHODS

The Support Vector Machine

Let x_i be a local sequence window centered on the interested cysteine or other sequence coding vectors (see the next section), and let y_i denote the state of the cysteine, either bonded ($y_i = 1$) or nonbonded ($y_i = -1$). The SVM technique tries to find the separating hyperplane $w^T x_i + b = 0$ with the largest distance between two classes, measured along a line perpendicular to this hyperplane. However, it happens that these data to be classified may not be linearly separable. To overcome this difficulty, the SVM nonlinearly transforms the original input space into a higher dimensional feature space by $\phi(x) = [\phi_1(x), \phi_2(x), \dots]$ and tries to minimize $\frac{1}{2} w^T w + C \sum_{i=1}^l \xi_i$ with respect to w, b

Grant sponsor: National Science Council in Taiwan, Republic of China (to J.-K. Hwang).

*Correspondence to: Jenn-Kang Hwang, Department of Biological Science and Technology, National Chiao Tung University, Hsinchu 30050, Taiwan, ROC. E-mail: jkhwang@cc.nctu.edu.tw

Received 22 September 2003; Accepted 4 December 2003

Published online 16 April 2004 in Wiley InterScience (www.interscience.wiley.com). DOI: 10.1002/prot.20079

and ξ under the constraint that $y_i[w^T \phi(x_i) + b] \geq 1 - \xi_i$, where $\xi_i \geq 0$. To solve the above equations, we need a closed form of $K(x_i, x_j) \equiv \phi(x_i)^T \phi(x_j)$, which is usually called the kernel function. In this work, we use the radial basis function (RBF) kernel: $e^{-\gamma \|x_i - x_j\|^2}$, where γ is a parameter. It should be noted that only some of the x_i 's are used to construct w and b , and these data are called support vectors.

The Feature Vectors Sequence input vector

The sequence input vector is defined by n flanking residues of the interested cysteine. Each residue in the sequence is encoded as a vector of 20 binary elements. It is easy to extend this coding scheme to include evolutionary information such as the homologous sequence profiles.^{28,29} We use the notation $x_s(w)$ to denote the sequence input vector enclosing a window of size w . The binary coding scheme does not give an explicit description of the physicochemical properties of the amino acids. To take these properties into consideration, we follow the approach recently developed by Meiler et al.,³⁰ which describes the amino acids in terms of five parameters: graph shape index, polarizability, volume, hydrophobicity, and isoelectric point. The graph shape index is calculated directly from the graph structure of the amino acid side-chain, which contains information about complexity, branching, and symmetry of the group; the hydrophobicity is defined as $\log P$ (amino acid) $- \log P$ (glycine), where P is the partition coefficient of the amino acid in octanol/water. The volume parameter is defined as the ratio of the van der Waals volume of the side-chain to that of CH_2 group. The polarizability is related to the molar refractivity. We use the notation $x_r(w)$ to denote this type of sequence representation.

Composition input vector

The composition input vector is composed of 20 elements, each of which corresponds to the compositional percentage of an amino acid of type a in a sequence window. The amino acid composition is given by $x_a = n^a/w$, where n^a is the number of occurrences of the amino acid of type a in the sequence window of size w . It is easy to implement evolutionary information from the homologous sequence profiles²⁸. For N multiple sequence alignments, the composition of the amino acid of type a is computed by $\sum_i^N n_i^a / \sum_i^N w_i$, where w_i is the size of the i th sequence window and n_i^a is the number of amino acids of type a of the i th sequence. We use the notation $x_c(w)$ to denote the composition-coding scheme and x_{c_0} for the full-length sequence composition. We ignore gaps in the multiple sequence alignment.

Data Sets

We use the data set of Martelli et al.,¹⁹ which comprises 4136 cysteine-containing segments (1446 are in the disulfide-bonded states, and 2690 are in the non-disulfide-bonded states). These segments are extracted from 969 nonhomologous proteins (sequence identity $< 25\%$ and

without chain breaks) from the Protein Data Bank (PDB).³¹ In this data set, the cysteines involved in interchain disulfide bonding are treated as "free" cysteines.

The Cysteine State Sequence

Each cysteine has two possible states: the bonding state and the nonbonding state. Since the bonding cysteines have to appear in pairs (we exclude the interchain disulfide bridges), the number of combinations is actually 2^{n-1} . For example, for proteins with 3 cysteines, there are $2^{3-1} = 4$ cysteine state sequences (CSSs) [i.e., (*OO*), (*OR*), (*RO*), and (*RR*)], where *O* and *R* designate the bonding and nonbonding states of the cysteine, respectively. Each CSS provides a transition path of a particular type of the bonding states of all cysteines in a chain. If the probabilities of the related states (*O* or *R*) and the transition probabilities from one state to another are known, the probability of the particular transition path can be easily computed. Comparison of the probabilities of the transition paths allows one to predict the most probable CSS. Thus, CSS description provides global information about the bonding states of the cysteines, which is complementary to local information of cysteines provided by the sequence input vector. Formally, for a protein with n cysteines, we describe the CSS by the vector $\mathbf{s}_n = (\sigma_0, \sigma_1, \sigma_2, \dots, \sigma_n, \sigma_{n+1})$, where $\sigma_i \in \{O, R\}$, $\sigma_0 = S$, and $\sigma_{n+1} = F$, denoting the initial and the final state³² of the sequence, respectively. For each \mathbf{s}_n , there is an associated transition probability vector $(\tau_0, \tau_1, \dots, \tau_n)$, where τ_i is the state-to-state transition probability from σ_i to σ_{i+1} . Let π_{σ_i} be the state probability of the i th cysteine in state σ_i ; then the transition probability of the CSS vector \mathbf{s}_n is given by $\tau_0 \prod_{i=1}^n \pi_{\sigma_i} \tau_i$. The state probability of the i th cysteine state π_{σ_i} in state σ_i is evaluated by normalizing the decision value x obtained from SVM by the arctan transfer function given by

$$f(x) = \{[a \tan^{-1}(bx)] + \pi/2\}/\pi,$$

where a and b are parameters, and $0 \leq a \leq 1$. In this work, all SVM calculations are performed using LIBSVM,³³ a general library for support vector classification and regression.

Optimization of CSS by the Branch-and-Bound Method

We use the branch-and-bound algorithm to optimize the probability of CSS, that is, $\max\{\tau_0 \prod_1^n \pi_{\sigma_i} \tau_i\}$. The procedures proceed as follows: We set an initial candidate CSS, \mathbf{s}_{init} , which is obtained from SVM. If the number of the bonded cysteines is odd, we simply reverse the state of last cysteine so that the number of the bonded cysteines is even. The probability is given by $p_{init} = \tau_0 \prod_0^n \pi_{\sigma_i}$. We then scan the CSS sequentially from (*R, R, ..., R*) to (*O, O, ..., O*). The probability of the given CSS sequence \mathbf{s}_n that includes the first m cysteines is computed by $p_m(\mathbf{s}_n) = \tau_0 \prod_1^m \tau_i \pi_{\sigma_i}$. If $p_m < p_{init}$, then \mathbf{s}_n is rejected, and we go on to the next CSS sequence. If $p_m \geq p_{init}$, we compute $p_{m+1} = \pi_{\sigma_{m+1}} \tau_{m+1} p_m$ and continue the comparison. If the final probability $p_n(\mathbf{s}_n) > p_{init}$, then this CSS sequence \mathbf{s}_n will be used as the

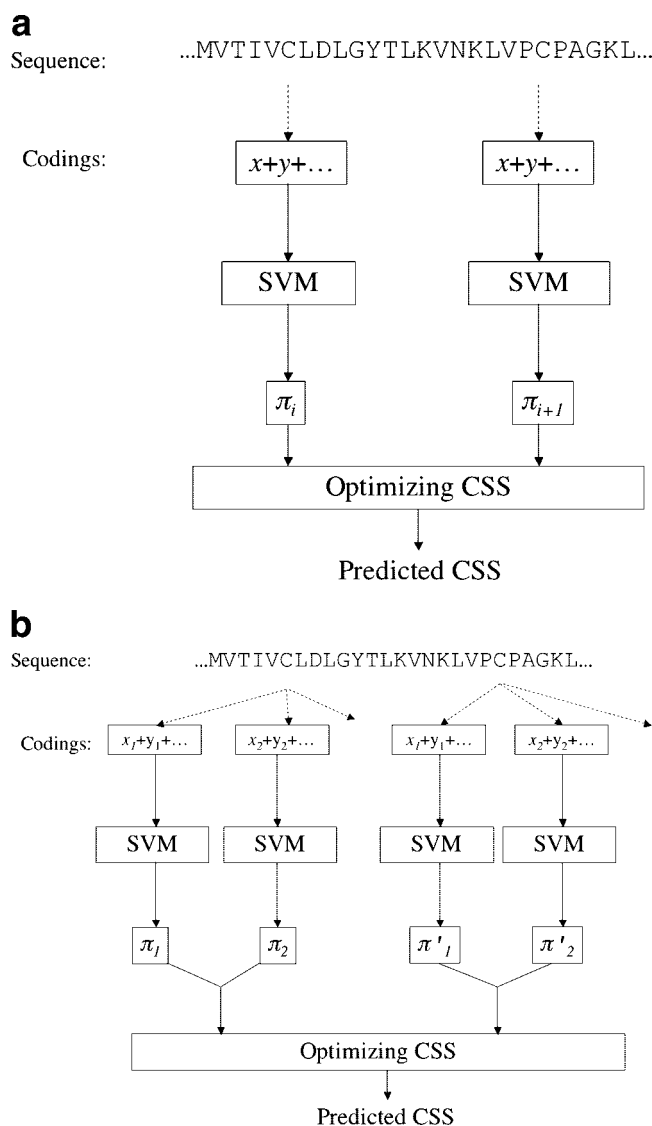


Fig. 1. (a) The single SVM trained with multiple feature vectors denoted by $x + y + \dots$ generates the state probability π_i for the given cysteine. The resultant CSS transition probabilities are then optimized to generate the predicted CSS. (b) The multiple SVM trained with different feature vectors ($x_1 + y_1 + \dots$ or $x_2 + y_2 + \dots$) to generate an average probability π_i for the given cysteine. The CSS optimization is identical with the previous method.

new candidate sequence. The whole process continues until we find the best CSS.

We use two different approaches that combine SVM and CSS. Figure 1 schematically shows the outlines. The first approach [Fig. 1(a)] uses a single SVM that is trained with multiple feature vectors denoted by $x + y + \dots$ to produce state probability π for the given cysteine. We then optimize the resultant CSS to generate the final prediction for the bonding states of the cysteines. The second approach [Fig. 1(b)] uses multiple SVMs trained with different feature vectors to generate averaged state probabilities for the given cysteine. The optimization procedures are identical with the first method. In this article, we use the notation $\{x + y + \dots\}$ to denote the SVM trained with input

vector $x + y + \dots$, and the notation $\{x + y + \dots\} + \text{CSS}$ to denote the SVM classifier $\{x + y + \dots\}$ coupled with CSS.

The Transition Probabilities of the Cysteine State Sequences

Figure 2 shows the observed state-to-state transition probabilities of proteins with 3–6 cysteines obtained from the data set of 969 nonhomologous proteins. For proteins with odd number cysteines [Fig. 2(a and c)], the first cysteines are predominately in the nonbonded form (the state probabilities for 3-cysteine and 5-cysteine proteins are 0.93 and 0.90, respectively). On the other hand, for proteins with an even number of cysteines [Fig. 2(b and c)], the first cysteines do not have as strong a tendency to be nonbonded—the probabilities for 4-cysteine and 6-cysteine proteins are 0.55 and 0.53, respectively. We observe that, in general, for a cysteine of a given state, the following cysteine has a strong tendency to be an identical state. Similar results have also been reported.¹⁵ It is possible to determine the full states of cysteines from the knowledge of the states of the first few cysteines. For examples, given the states of the first 2 cysteines, (O, R), of proteins with 5 cysteines, we can predict the rest of the cysteines to be (O, O, O), and in the case of proteins with 6 cysteines, the states of the following cysteines are (R, O, O, O). The CSSs are useful in revealing global correlation between the cysteine states. Note that the transition probabilities of some states depend on more than their immediate previous states, which does not conform to the Markov memory-less condition. It is obvious that the Markov model is not the best model for the CSS; however, the Markov model may be still useful in describing the global bindings states of cysteines when complemented with local information of cysteines. In practice, we try to optimize the state-to-state transition probabilities through the following processes: The proteins in the database are classified into 24 groups based on their cysteine numbers, and the average transition probabilities of the state-to-state transitions are computed for each group. We classify the transition paths into 12 types, namely, (S, O_1), (S, R_1), (O_1, O_2), (O_2, O_1), (R_1, R_1), (R_2, R_2), (R_1, O_1), (R_2, O_2), (O_1, R_2), (O_2, R_1), (R_1, F), and (O_2, F). Here O_1 and O_2 designate the first and second cysteine of the cysteine bridge, respectively. R_1 and R_2 are the nonbonded cysteines before the first and second cysteines that form a disulfide bridge. The transition probabilities are obtained by averaging the transition probabilities over these transition paths. In this way, we consider the protein groups as 24 nodes in a 12-dimensional space. We calculate the Euclidian distances among these nodes and cluster the groups by the neighbor-joining method.³⁴ The protein clusters with less than 8 proteins were combined with their clustered neighbors to ensure that each cluster contains enough number of proteins.

Assessment of the Prediction Accuracy

Our assessment of the prediction accuracy follows the standard convention¹⁸. The overall prediction accuracy Q_2 is evaluated as $Q_2 = N_c/N_0$, where N_c and N_0 are the total number of correct predictions for the bonded cysteines and

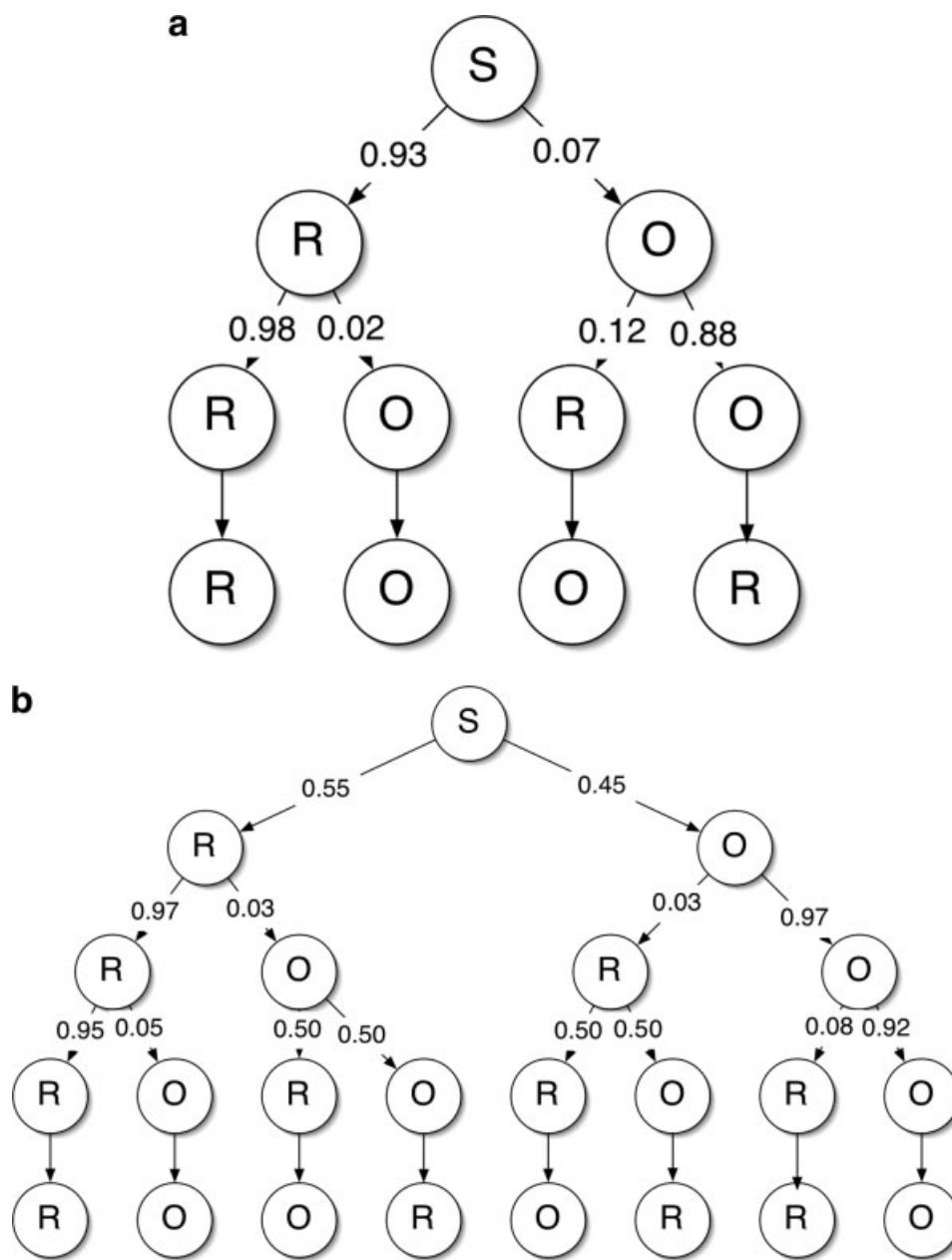


Fig. 2. The observed CSSs evaluated from 969 nonhomologous proteins from the PDB (see Data Sets in Methods section). The notations *S*, *O*, and *R* denote the initial, bonding, and nonbonding states, respectively. The arrows indicate the transition path from one state to another, and the numbers labeled indicate the corresponding transition probabilities (for clarity, the unit transition probability is not labeled). Four examples of the observed CSSs are shown: disulfide proteins with (a) 3 cysteines, (b) 4 cysteines, (c) 5 cysteines, and (d) 6 cysteines.

the total number of the bonded cysteines, respectively. The specificity (*spec*; i.e., the fraction of all positive predictions that are true positives) is given by

$$spec = \frac{TP_x}{TP_x + FP_x}, \quad x = SS \text{ or } SH,$$

where FP_x is the number of false negatives or overpredictions. The sensitivity (*sens*; i.e., the fraction of positive

examples predicted) for the bonded cysteine (*SS*) or the nonbonded cysteine (*SH*) is given by

$$sens = \frac{TP_x}{TP_x + FN_x}, \quad x = SS \text{ or } SH,$$

where TP_x is the number of true positives for state x , and FN_x is the number of false negatives or underpredictions. The Matthews correlation coefficient (MCC)³⁵ is given by

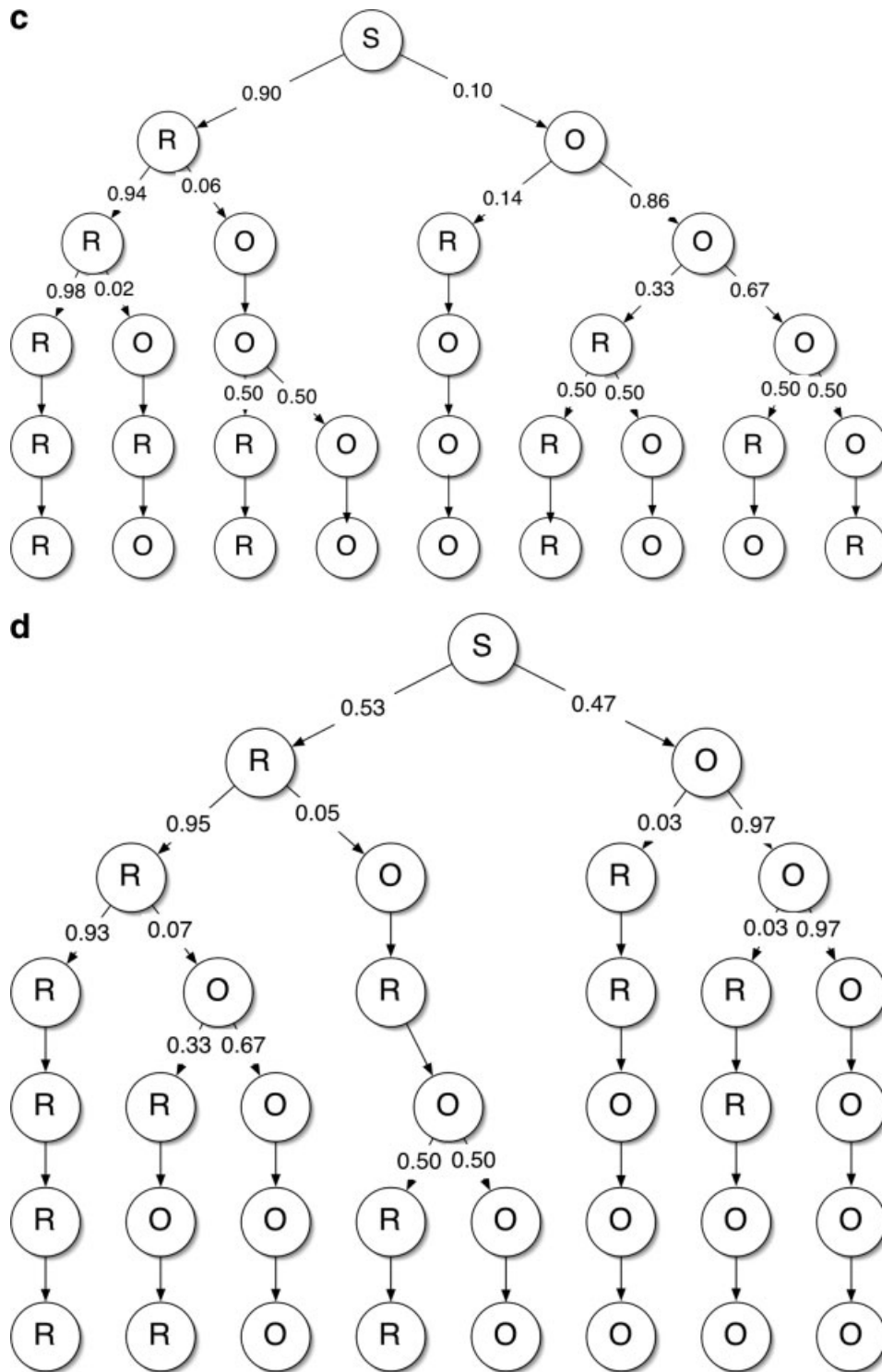


Figure 2. (Continued)

$$MCC = \frac{TP_x TN_x - FP_x FN_x}{\sqrt{(TP_x + FN_x)(TP_x + FP_x)(TN_x + FP_x)(TN_x + FN_x)}},$$

$x = SS \text{ or } SH,$

where TN_x is the true negatives of state x . The value of MCC_x is 1 for a perfect prediction, and 0 for a completely random assignment. All the results reported here are from 20-fold cross-validation.

TABLE I. Predictive Performance of SVM Based on Sequence Inputs of Different Window Lengths, $\{x_s(w)\}$

Window length	Q_2	MCC	SS		SH	
			<i>spec</i>	<i>sens</i>	<i>spec</i>	<i>sens</i>
5	0.75	0.46	0.69	0.63	0.78	0.82
9	0.79	0.54	0.71	0.69	0.84	0.84
13	0.80	0.56	0.71	0.71	0.85	0.84
15	0.81	0.58	0.71	0.73	0.87	0.84
17	0.80	0.56	0.71	0.72	0.86	0.84
21	0.80	0.55	0.69	0.72	0.86	0.83

TABLE II. Predictive Performances of SVMs Based on Composition Inputs of Different Window Lengths, $\{x_c(w)\}$

Window length	Q_2	MCC	SS		SH	
			<i>spec</i>	<i>sens</i>	<i>spec</i>	<i>sens</i>
9	0.67	0.22	0.29	0.59	0.88	0.69
15	0.70	0.31	0.41	0.62	0.87	0.73
25	0.73	0.38	0.46	0.67	0.89	0.75
35	0.75	0.42	0.51	0.69	0.89	0.76
Full length	0.80	0.55	0.65	0.75	0.88	0.82

TABLE III. Comparison of Predictive Performances of SVM Based on Single and Multiple Feature Vectors

Methods	Q_2	MCC	SS		SH	
			<i>spec</i>	<i>sens</i>	<i>spec</i>	<i>sens</i>
$\{x_s(15)\}$	0.81	0.58	0.71	0.73	0.87	0.84
$\{x_{c0}\}$	0.80	0.55	0.65	0.75	0.88	0.82
$\{x_s(7) + x_{c0}\}$	0.86	0.69	0.79	0.75	0.89	0.89

RESULTS AND DISCUSSION

In Table I, we compare the predictive performances of $\{x_s(w)\}$ (i.e., SVMs based on local sequence feature vectors of different window sizes). The predictive performances steadily increases in accordance with the window size, and reach the maximum ($Q_2 = 81\%$) when the window size is 15. The prediction accuracy remains relatively the same as the window size increases. Similar prediction accuracy was also observed in studies using other approaches based on local sequence feature vectors.^{16,18} In Table II, we compare the predictive performances of $\{x_c(w)\}$ (i.e., SVMs based on composition input vectors of different window sizes). The predictive performance increases dramatically as the window size increases, and reaches the maximum $Q_2 = 80\%$ at the full length. The increase of prediction accuracy mainly comes from improvement on the sensitivity of SS (from 0.29 to 0.65). The surprisingly high accuracy using only a 20-element input vector (i.e., 20 compositions of amino acids) is consistent with the observation that cysteines of the protein prefer to be in only one state, either bonding or nonbonding.

Table III compares results based on single or multiple feature vectors. The SVM classifier $\{x_s(7) + x_{c0}\}$ gives $Q_2 = 86\%$ and MCC = 0.69, significantly improving on either $\{x_s(15)\}$ ($Q_2 = 81\%$) or $\{x_{c0}\}$ ($Q_2 = 80\%$). The combined SVM classifier $\{x_s(7) + x_{c0}\}$ considerably increases the MCC

TABLE IV. Comparison of Predictive Performances of SVMs Coupled with CSS

Methods	Q_2	MCC	SS		SH	
			<i>spec</i>	<i>sens</i>	<i>spec</i>	<i>sens</i>
$\{x_s(15)\} + \text{CSS}$	0.89	0.74	0.91	0.74	0.87	0.97
$\{x_s(7) + x_{c0}\} + \text{CSS}$	0.88	0.71	0.88	0.74	0.87	0.95
$\{x_s(7) + x_r(7)\} + \text{CSS}$	0.88	0.73	0.89	0.74	0.87	0.95
Multiple SVM + CSS ^a	0.90	0.77	0.91	0.77	0.89	0.97

^aThe multiple SVM classifiers are $\{x_s(15)\}$, $\{x_s(7) + x_{c0}\}$, and $\{x_s(7) + x_r(7)\}$.

value for bonded cysteines (from 0.58 or 0.55 to 0.69). Since $\{x_{c0}\}$ will fail in the case of proteins with mixed bonding states of cysteines and $\{x_s(15)\}$ does not know of the global "all-or-none rule" for bonded (or nonbonded) cysteines, a combination of local environment, $x_s(w)$, and global properties, x_{c0} , can better capture essential features of cysteine states.

Table IV lists the results obtained from SVMs coupled with CSS, which carries information about the global patterns of the cysteine states in proteins. When the SVM is coupled with CSS, we consistently obtain the overall prediction accuracy Q_2 ranging from 88% to 90%, and MCC from 0.71 to 0.77. Just like a global property such as the amino acid composition, CSS can help significantly increase prediction accuracy. For example, $\{x_s(15)\} + \text{CSS}$ yields prediction accuracy $Q_2 = 89\%$, about 8% higher than that of $\{x_s(15)\}$. In the case of $\{x_s(7) + x_{c0}\}$, which includes global property in terms of the amino acid compositions, the effects of CSS are not as pronounced as the previous example on increasing prediction accuracy (Q_2 from 86% to 88%). We also notice that the SVM+CSS significantly increases the specificity in predicting bonded cysteines ranging from 88% to 91%, compared with that of SVM based on local sequence windows (*spec* = 71% for SS). Combining multiple SVM classifiers coupled with CSS, we are able to obtain the best predictor: $Q_2 = 90\%$ and MCC = 0.77.

CONCLUSIONS

We have developed an approach to predict the bonding states of cysteine using SVM methods based on the local sequence windows and global descriptors such as the total amino acids and the cysteine state sequences. We found that the SVM method based on the combined local sequence windows and global amino acid compositions significantly improves the predictive performances. Obviously, the combination of local environments of cysteines (such as local sequence windows) and global properties (such as total amino acid compositions) can better capture essential features of cysteine states. Coupled with CSS, SVM based on multiple-feature vectors yields 90% prediction accuracy and 0.77 MCC, considerably higher than the corresponding values 81% and 0.58, respectively, obtained by SVM based on local sequence windows. We also notice that the SVM+CSS significantly increases the specificity in predicting bonded cysteines (88–91%), around 20% higher than that of SVM based on local sequence windows. Higher

specificity in bonded cysteines allows for confident prediction and prevents error propagations. Though we did not include structural information in our input vectors, it is possible to include structural information, such as the predicted secondary structures or the predicted solvent accessible areas of the cysteines, as well as the flanking residues in the windowing.

Our study shows that the bonding state of the cysteines is determined by both the local information of the particular cysteine, such as the flanking amino acid sequences, and the global information, such as the composition content of the proteins, as well as the bonding states of other cysteines. Our results may be useful in both protein modeling^{12,36} and protein engineering.³⁷ Recently, there have been efforts to enhance the stability of proteins by introducing engineered disulfide bonds,^{38–40} and our results may also be useful in suggesting appropriate residues for disulfide crosslinking.

REFERENCES

- Clark J, Fersht A. Engineered disulfide bonds as probes of the folding pathway of barnase—increasing the stability of proteins against the rate of denaturation. *Biochemistry* 1993;32:4322–4329.
- Hwang J-K, Pan J-J. Classical trajectory mapping approach for simulations of classical reactions in solution and in enzymes. *J Phys Chem* 1996;100:909–912.
- Akamatsu Y, Ohno T, Hirota K, Kagoshima H, Yodoi J, Shigesada K. Redox regulation of the DNA binding activity in transcription factor PEBP2: the roles of two conserved cysteine residues. *J Biol Chem* 1997;272:14497–14500.
- Abkevich VI, Shakhovich EI. What can disulfide bonds tell us about protein energetics, function and folding: simulations and bioinformatics analysis. *J Mol Biol* 2000;300:975–985.
- Clarke J, Hounslow AH, Bond CJ, Fersht AR, Daggett V. The effects of disulfide bonds on the denatured state of barnase. *Protein Sci* 2000;9:2394–2404.
- Wedemeyer WJ, Welker E, Narayan M, Scheraga HA. Disulfide bonds and protein folding. *Biochemistry* 2000;39:4207–4215.
- Yokota A, Izutani K, Takai M, Kubo Y, Noda Y, Koumoto Y, Tachibana H, Segawa S. The transition state in the folding-unfolding reaction of four species of three-disulfide variant of hen lysozyme: the role of each disulfide bridge. *J Mol Biol* 2000;295:1275–1288.
- Gladyshev VN. Thioredoxin and peptide methionine sulfoxide reductase: convergence of similar structure and function in distinct structural folds. *Proteins* 2002;46:149–152.
- Anfinsen C, Scheraga HA. Experimental and theoretical aspects of protein folding. *Adv Protein Chem* 1975;29:205–300.
- Vielle C, Zeikus G. Hyperthermophilic enzymes: sources, uses, and molecular mechanisms for thermostability. *Microbiol Mol Biol Rev* 2001;65:1–43.
- Hogg PJ. Disulfide bonds as switches for protein function. *Trends Biochem Sci* 2003;28:210–214.
- Chuang CC, Chen CY, Yang J-M, Lyu PC, Hwang J-K. Relationship between protein structures and disulfide-bonding patterns. *Proteins* 2003;53:1–5.
- Muskal SM, Holbrook SR, Kim SH. Prediction of the disulfide-bonding state of cysteine in proteins. *Protein Eng* 1990;3:667–672.
- Fiser A, Cserzo M, Tudos E, Simon I. Different sequence environments of cysteines and half cysteines in proteins: application to predict disulfide forming residues. *FEBS Lett* 1992;302:117–120.
- Fiser A, Simon I. Predicting the oxidation state of cysteines by multiple sequence alignment. *Bioinformatics* 2000;16:251–256.
- Martelli PL, Fariselli P, Malaguti L, Casadio R. Prediction of the disulfide bonding state of cysteines in proteins with hidden neural networks. *Protein Eng* 2002;15:951–953.
- Muccielli-Giorgi MH, Hazout S, Tuffery P. Predicting the disulfide bonding state of cysteines using protein descriptors. *Proteins* 2002;46:243–249.
- Fariselli P, Riccobelli P, Casadio R. Role of evolutionary information in predicting the disulfide-bonding state of cysteine in proteins. *Proteins* 1999;36:340–346.
- Martelli PL, Fariselli P, Malaguti L, Casadio R. Prediction of the disulfide-bonding state of cysteines in proteins at 88% accuracy. *Protein Sci* 2002;11:2735–2739.
- Krogh A, Riis SK. Hidden neural networks. *Neural Comput* 1999;11:541–563.
- Vapnik V. The nature of statistical learning theory. New York: Springer; 1995.
- Jaakkola T, Kiekhans M, Haussler D. Using the Fisher kernel method to detect remote protein homologies. *Intel Syst Mol Biol* 1999;149–158.
- Brown MP, Grundy WN, Lin D, Cristianini N, Sugnet CW, Furey TS, Ares MJ, Haussler D. Knowledge-based analysis of microarray gene expression data by support vector machine. *Proc Natl Acad Sci USA* 2000;97:262–267.
- Dingg CHQ, Dubchak I. Multi-class protein fold recognition using support vector machines and neural networks. *Bioinformatics* 2001;17:349–358.
- Hua S, Sun Z. A novel method of protein secondary structure prediction with high segment overlap measure: support vector machine approach. *J Mol Biol* 2001;308:397–407.
- Yu C-S, Wang J-Y, Yang J-M, Lyu PC, Lin C-J, Hwang J-K. Fine grained protein fold assignment by support vector machines using generalized *n* peptide coding schemes and jury voting from multiple-parameter sets. *Proteins* 2003;50:531–536.
- Yu C-S, Lin C-J, Hwang J-K. Predicting subcellular localization of proteins for Gram-negative bacteria by support vector machines based on *n*-peptide composition. *Protein Science* 2004 (in press).
- Schneider R, Sander C. Database of homology-derived structures and the structural meaning of sequence alignment. *Proteins* 1991;9:56–58.
- Rost B, Sander C. Prediction of protein secondary structure at better than 70% accuracy. *J Mol Biol* 1993;232:584–599.
- Meiler J, Muller M, Zeidler A, Schmaschke F. Generation and evaluation of dimension-reduced amino acid parameter representations by artificial neural networks. *J Mol Model* 2001;7:360–369.
- Berman HM, Westbrook J, Feng Z, Gilliland G, Bhat TN, Weissig H, Shindyalov IN, Bourne PE. The Protein Data Bank. *Nucleic Acids Res* 2000;28:235–242.
- Durbin R, Eddy SR, Krogh A, Mitchison G. *Biological sequence analysis*. New York: Cambridge University Press; 1998.
- Chang C-C, Lin C-J. LIBSVM: a library for support vector machines. 2001. Software available from <http://www.csie.ntu.edu.tw/~cjlin/libsvm>.
- Saitou N, Nei M. The neighbor-joining method: a new method for reconstructing phylogenetic trees. *Mol Biol Evol* 1987;4:406–425.
- Matthews BW. Comparison of the predicted and observed secondary structure of T4 phage lysozyme. *Biochim Biophys Acta* 1975;405:442–451.
- Harrison PM, Sternberg MJE. The disulfide beta-cross: from cystine geometry and clustering to classification of small disulfide-rich protein folds. *J Mol Biol* 1996;264:603–623.
- Yokota A, Izutani K, Takai M, Kubo Y, Koumoto Y, Tachibana H, Segawa S. The transition state in the folding-unfolding reaction of four species of three-disulfide variant of hen lysozyme: the role of each disulfide bridge. *J Mol Biol* 2000;295:1275–1288.
- Hinck AP, Truckses Dm, Markley JL. Engineered disulfide bonds in staphylococcal nuclease: effects on the stability and conformation of the folded protein. *Biochemistry* 1996;35:10328–10338.
- Mansfeld J, Vriend G, Dijkstra BW, Veltman OR, Van den Burg B, Venema G, Ulbrich-Hoffmann R, Eijssink VG. Extreme stabilization of a thermolysin-like protease by an engineered disulfide bond. *J Biol Chem* 1997;272:11152–11156.
- Shimaoka M, Lu C, Salas A, Xiao T, Takagi J, Springer TA. Stabilizing the integrin alpha M inserted domain in alternative conformations with a range of engineered disulfide bonds. *Proc Natl Acad Sci USA* 2002;99:16737–16741.